Second harmonic generation from oxazine dyes at the air/water interface

Daniel A. Steinhurst[‡] and Jeffrey C. Owrutsky[*]

Code 6111, US Naval Research Laboratory
Washington, DC 20375-5342
Fax: (202) 404-8119

Abstract

Several oxazine laser dyes have been studied at the air/water interface by the surface-specific technique of second harmonic generation (SHG) spectroscopy. Oxazine 720, cresyl violet, and nile blue readily form H-aggregate type dimers in aqueous solutions. We report an SHG study of the air/water interface of aqueous solutions of these water-soluble dyes in which it appears that the SHG signals originate almost exclusively from the dimers. The dominance of the dimer in the SHG process holds over a wide range of dye concentration and monomer-to-dimer ratios. The measurements were carried out with incident laser wavelengths near 600 nm, which are resonant with the first electronic transition, and include SHG spectra, solution composition dependence (i.e. dye concentration, salt (NaCl), surfactant, etc.), and polarization dependence. Addition of salt to the dye solutions increases the observed SHG signal intensity to a much greater extent (by as much as a factor of 30) than it promotes bulk aggregation. The SHG polarization dependence, *i.e.*, the molecular orientation, remains unchanged. This suggests that the dimer concentration increases at the surface with the solution bulk ionic strength to a greater extent than for the bulk solution. The high concentration of dimers at the surface is consistent with the results of previous studies that reveal the less polar nature of the air/water interface relative to bulk water.

[‡] NRL-NRC Research Associate, e-mail: das@ccs.nrl.navy.mil
[*] Corresponding author, e-mail: jeff.owrutsky@nrl.navy.mil

Introduction

The chemical interface represents a unique environment sandwiched in between two bulk chemical environments that is clearly different than either bulk environment. Second harmonic (SHG) and sum frequency (SFG) generation techniques are well established and popular methods that have provided a great deal of new insight into the physical and chemical nature of the various types of interfaces.[1-11] One advantage of nonlinear optical surface studies is that they provides a way to study interfaces that are not accessible by traditional surface science methods, such as electron spectroscopies, outside the vacuum environment. For studies of monolayer films, such as Langmuir-Blodgett films on liquids and thin molecular films on solid surfaces, linear spectroscopic methods, such as transmission and reflection spectroscopy and ellipsometry can be employed, but SHG is a complementary approach. For investigating species with a measurable solubility in the bulk, the bulk contribution often precludes the use of linear spectroscopic approaches to measure surface properties. Consequently, the surface specificity afforded by SHG spectroscopy provides perhaps the only optical method to study the molecular structure and dynamics, as in the case of oxazine dyes at the air/water interface investigated here.

SHG has been used extensively to investigate adsorbates at various types of interfaces. Second order nonlinear optical mixing processes such as SHG are dipole forbidden in centro-symmetric media, but the very nature of the interface provides a break in the long-range symmetry of the bulk and allows SHG to occur. The intensity of the SHG signal generated at an interface, I_{SHG}, is given by the relation[12,13]

$$I_{\mathrm{SHG}} = \frac{32\pi^3\omega^2 \sec^2\theta}{Ac^3}\left|\hat{e}^{2\omega}\cdot\boldsymbol{\chi}^{(2)}\cdot\hat{e}^{\omega}\hat{e}^{\omega}\right|^2 I_{\omega}^2 \qquad (1)$$

where I_ω and I_{SHG} indicate the intensities at the fundamental and the second harmonic frequencies, respectively, θ is the angle between the surface normal and the propagation direction of the second harmonic, $\boldsymbol{\chi}^{(2)}$ is the second-order nonlinear susceptibility, $\hat{e}$ is a vector quantity related to the electric field of the referenced beam and A is the irradiated area. The nonlinear susceptibility $\boldsymbol{\chi}^{(2)}$ and the observed SHG signal can be enhanced if the incident or generated radiation is resonant with a molecular transition for an adsorbate at the interface at the fundamental frequency (ω) or at the resulting second harmonic frequency (2ω). If the substrate response and non-resonant molecular terms are small by comparison, $\boldsymbol{\chi}^{(2)}$ can be expressed as [14]

$$\boldsymbol{\chi}^{(2)}(\omega) \propto \frac{\mu_{01}\mu_{12}\mu_{02}N_s}{(\omega_{10}-\omega+i\Gamma_{10})(\omega_{20}-2\omega+i\Gamma_{20})} \qquad (2)$$

where N_s represents the surface concentration, μ_{01}, μ_{12}, and μ_{12} are the linear transition dipole moments for transitions $0\rightarrow1$, $1\rightarrow2$, $0\rightarrow2$, and ω_{n0} and Γ_{n0} are the transition frequency and dephasing rate for transitions from the ground state to states $n = 1, 2$.

Results from SHG studies have yielded information about equilibria and molecular structure for interfaces and adsorbates.[1-20] For example, some properties for air/liquid interfaces, such as polarity, as indicated from measured solvent shifts,[15,16] are close to the average of the two bulk phase values. Several studies, including those of surface *pK*, suggest that charged species are not easily accommodated at the surface.[18-20] For some dynamical process, such as isomerization and rotational reorientation, the rates at the interface depend on specifics of the adsorbate geometry, interfacial solvation and the molecular motion. For

example, rotational relaxation was measured to be slower for malachite green (MG)[21] and rhodamine 6G (R6G)[22] at air/liquid interfaces but faster for eosin B.[23]

Aggregation is well known to take place for many cationic dyes in water and has been more extensively studied on solid surfaces or for insoluble films than for soluble species at the air/water interface. Dye aggregates are an integral component of many imaging and light conversion applications such as photography[24,25] and solar energy conversion.[26,27] They are used to sensitize semiconductor materials such as silver bromide nanocrystals for color photography by adjusting the large bandgap of the semiconductor. Aggregates have also been used in the photocatalytic remediation of waste water streams.[28,29]

The exciton theory of dipole-dipole coupling can be used to relate the distance and relative orientation of monomeric dye molecules within an aggregate to the electronic structure and to the resulting spectral shifts (and transition moments) of the aggregate.[30-33] For a dimer composed of two monomer units with parallel transition moments, the first excited singlet energy levels of the dimer are split into two levels, one lower (S^-) and one higher (S^+) in energy than the first excited singlet state of the separated monomers. The allowed transitions and observed dimer band position relative to the monomer depend on Θ, the angle between the center of separation and the monomer transition moments. For "sandwich-type" H-aggregates, $54.7^\circ \leq \Theta \leq 90^\circ$ (at $\Theta = 90^\circ$, the monomer dipole moments are aligned parallel), and only transitions to the S^+ energy level are allowed and the resulting absorption band is blue shifted from the monomer. For J-aggregates, $\Theta < 54.7^\circ$ (at 0°, the monomer dipole moments are aligned end-to-end), only transitions to the S^- energy level are allowed and the absorption band is red shifted.[30-33] For H-aggregates there is rapid internal

conversion of population in the S^+ energy level to the S^- singlet level, such that the fluorescence is greatly reduced as reported for cresyl violet.[34-36]

The aggregates of the oxazine laser dyes have been a focus of research owing to the potential industrial applications of the aggregate's strong absorption bands in the visible. The physical properties of the oxazine dye family have been extensively studied due to the long-term stability and the high quantum yields of the oxazine dyes as laser dyes. The structures of nile blue, cresyl violet and oxazine 720 are shown in Figure 1. Gvishi and Reisfeld[37] reported a dimer equilibrium constant ($K_d = [M]^2/[D]$) for oxazine 720 (170) [38] in aqueous solution of $K_d = 2.0 \pm 0.5 \times 10^{-5}$ M. Herkstroeter et al.[35] reported that the dimer equilibrium constant was several orders of magnitude higher for oxazine 720 than for oxazine 725 (1). Oxazine 725 and LD690 (oxazine 4) have a different backbone structure than nile blue, cresyl violet and oxazine 720; the former two are missing the fourth aromatic ring that breaks the C_{2V} molecular symmetry. Consequently, these two molecules are less hydrophobic which is the most likely reason why they do not form dimers as readily. Herkstroeter et al.[35] also pointed out that a quantitative measurement of K_d for oxazine 720 was complicated by adsorption on the glass surfaces of the cells used; they did however report that K_d was in the range 10^{-4} - 10^{-5} M, which is consistent with the value of Gvishi and Reisfeld.[37] The relative propensity to form dimers for several dyes was reported by Morozova and Zhigalova:[39] nile blue > R6G > oxazine 725.

Adding various species to a solution can alter the dimer equilibrium constant. Surfactants can be used to dissociate dimers resulting in a dye solution consisting almost entirely of monomers.[40] The addition of salt to the solutions has been observed to cause changes in the extent of dye aggregation, or what is called the salt effect.[41] In measuring the

fluorescence quantum yield of cresyl violet in water, Isak and Eyring[36] observed that the addition of salt, in this case potassium iodide, enhanced the formation of aggregates at concentrations above 10^{-6} M and that the salt quenched the fluorescence of the dye solution. Nüesch and Grätzel[42] reported that adding NaCl (1.8 M) increases K_d by a factor of two for a mericyanine dye. Das et al.[43] studied the effect of salts on air/water adsorption of para-nitrophenol (PNP) using the SHG technique and pointed out that the effect depends on the specific salt used. Those with small electrolytes (LiCl, NaCl) exhibit a "salting out" effect which decreases the bulk solubility and ΔG_{ads}. Salts comprised of larger ions, such as $LiClO_4$ however, can have a "salting in" effect of increasing solubility and ΔG_{ads}. The salt effect was utilized by Levinger et al.[44] who measured surface SHG spectra at the air/water interface for the indocyanine dye / biological stain IR-125. The bulk spectra were altered by salt ($CaCl_2$), which induced the formation of aggregrates. The absorption shifts observed are more consistent with the formation of B-aggregates. Their resonantly enhanced near-infrared (NIR) SHG spectra resembled the bulk spectrum with salt, providing a way to identify that the aggregate is responsible for the surface SHG spectrum.

The properties of the oxazine dye aggregates at liquid/solid interfaces have been of interest for the last several decades. It was suggested some time ago that solar light harvesting with wide bandgap semiconductor photoconductors may be improved by covering the semiconductor with dyes to expand the wavelength range. Oxazine dyes have been identified as viable candidates and investigated for this purpose. One of the primary issues is the effect of dye aggregation at the solid/liquid interface and this has been studied recently for cresyl violet by Kamat and coworkers [45-48] and for nile blue by Nasr and Hotchandani,[49] both on SiO_2 and SnO_2 particles. The dyes form dimers (H-type aggregates) on the particles

in aqueous solution. The spectra reported for dimers at these solid/liquid interfaces are similar to those observed in bulk solution except for a small spectral shift to the blue on the SnO_2 particles. The measurements included ultrafast studies of the excited state dynamics as well as the measurement of electron transfer rates to the semiconductor support.

In this study we report SHG studies of nile blue (NB), cresyl violet (CV) and oxazine 720 (OX720) at the air/water interface. The results include measurements of the SHG spectra in the region near 600 nm, and the dependence of the SHG signal intensity on bulk solution composition and the input laser polarization. The oxazines are soluble in water, so the surface coverage is governed by the adsorption equilibrium between the surface and the solution which depends on the solution composition. The behavior of the dye at the surface can be compared to that in the bulk to provide information about the aqueous surface properties. Previous studies in this regard have been reported, such as those on aqueous surface adsorption kinetics, pK_a and polarity changes with respect to the bulk, and the results indicate that the air/water interface is less accommodating of charged or polar species than is the bulk.[2,7,15-20,43,50,51]

The SHG intensity depends on both the molecular orientation and concentration at the surface. The SHG polarization dependence can be used, typically accompanied by assumptions about the dominant hyperpolarizibilities and the orientation distribution function, to derive relative molecular hyperpolarizabilities and mean orientation angles for a species present at an interface. By measuring the SHG polarization dependence it should be possible to distinguish between orientational and concentration effects on any observed changes in the SHG signal intensity. Orientational information can also be determined for thin films on solids or liquids by polarization-resolved linear reflection or transmission

spectroscopy. There are numerous SHG orientation studies[1,2,4,13,19, 52-62] that have been reported, many of which have been the subject of several reviews.[6-10] Heinz et al. reported the measurement of the average orientation for rhodamine dyes on silica[1] and for *p*-nitrobenzoic acid at the air/silica and the ethanol/silica interfaces[2]. The polarization anisotropy of SHG measurements made on methylene blue, both chemisorbed[52] and physisorbed[53] on solid surfaces by Corn and coworkers showed the general ability of the SHG technique to provide orientational information for differing molecules and substrates even at sub-monolayer surface coverages. Recent studies of dyes on silica using SHG have been reported by Leach and coworkers.[54,55] and by Meech and Morgenthaler.[56] Studies by Eisenthal and et al.[22] and by Antoine et al.[23] have used SHG to measure rotational relaxation rates of molecules at the air/water interface. The solvation dynamics of courmarin 314 by Zimdars and coworkers[57,58] have shown that the relaxation times are dependent on the orientation of the molecule at the interface.

SHG results are reported here for aqueous solutions of several oxazine laser dyes. These dyes form aggregates in bulk solution and based on the results of the various SHG measurements we interpret the SHG signal as being almost entirely due to the dimers. This conclusion is consistent with previous observations for organic molecules at the air/water interface which indicate that hydrophobic species preferentially adsorb at the surface. Since the dimer is more hydrophobic than the monomer, it should be the preferred species residing at the surface.

Experimental

All laser dyes were obtained from Exciton as the perchlorate salt and were used without further purification. All solutions were prepared with deionized water and commercial grade NaCl without further purification. Bulk linear absorption spectra were recorded on a Hitachi U3000 recording spectrometer using a 0.2 cm thick quartz cell or a Spectral Instruments Model 420 CCD array spectrometer with a 1 cm path length dip probe.

A 6.3×10^{-4} M aqueous stock solution of each dye was prepared by adding solid dye to a volumetric flask, adding sufficient deionized water and sonicating the solution for 30 minutes. The effect on both the bulk aggregation and the surface SHG signal intensity for a variety of different solvents and additional solution components were studied. All compounds were of reagent grade or better and used without further purification. Methanol and ethanol solvents were used in addition to aqueous solutions. For additional solution components, two salts, sodium chloride (NaCl) and lithium chloride (LiCl), and two surfactants, Triton X-100 (Fisher Scientific), and polystyrene sulfonic acid (Polysciences, sodium salt) were used. For all measurements reported in this work, unless otherwise noted, the bulk solution is aqueous, any salt used is NaCl, and the surfactant is Triton X-100. The surfactant was added by transferring a small amount of the neat solution to the sample vial on the tip of a disposable pipet and stirring the solution.

The output of a Nd:YAG laser (532 nm, 10 Hz, 10 ns pulse width, Spectra-Physics DCR-2A) pumped dye laser (Quantel TDL-50) was used to produce tunable laser radiation over the wavelength range 560 – 660 nm for the second harmonic measurements. The laser dyes DCM, Rhodamine 590 (R6G), 610, and 640 (Exciton) in methanol were used in the dye

laser to provide the necessary wavelength coverage. Nanosecond pulse-width SHG measurements were made using pulse energies of 1 – 10 mJ. The 5 mm dia. unfocused laser beam was directed at the sample at incident angles of 33° and 60° with respect to the surface normal by a fused silica (FS) 90° prism. The fundamental and second harmonic (SH) light reflected from the surface were spatially filtered from any lower surface reflections and directed by a second FS prism into a FS Pellen-Broca prism to spatially disperse the fundamental and SH. Any remaining fundamental was removed by a color filter (Corning 7-54). The SH was sent into a 0.125 m monochromator (Jarrall-Ash) and a photomultiplier tube (PMT, RCA 1P28). Both the monochromator and additional color filters were used to discriminate between SH light and fluorescence from the bulk solution. The output from the PMT was sent to a digital oscilloscope (LeCroy 9400) and averaged for 200 - 500 shots. Signals were observed that were much broader spectrally than the SHG signal; these were attributed to two photon fluorescence and subtracted from the measured intensity to obtain the SHG signal.

In order to measure SHG spectra for wavelengths shorter than 560 nm, a Q-switched, mode-locked Nd:YAG laser pumped OPG/OPA (Continuum) was used. This system provided 100 μJ, 80 ps pulses at a 10 Hz repetition rate which are tunable over the range 450-700 nm. The laser beam was focused onto the sample with a 10 cm focal length lens.

For the study of bulk composition on the measured SHG signal intensity and the polarization anisotropy, a laser system producing 500 fs pulse width, 20 μJ pulses operating at a one kHz repetition rate was used. Tunable frequency pulses were generated by a homemade optical parametric amplifier (OPA) pumped by the frequency-doubled output (400 nm) of a regeneratively-amplified Ti:Sapphire laser system. The OPA is seeded by a

continuum pulse, which is generated by focusing a small fraction of fundamental (800 nm) into a 3.2 mm thick piece of sapphire. Tunable (530-680 nm) OPA pulses (≈ 20 μJ) are generated by combining the 400 nm pump and continuum pulses into a 0.4 mm, type I BBO crystal. The OPA pulses are separated with a color filter and a polarizing beam splitter cube and then focused with a 15 cm focal length lens on the sample. The same detection arrangement was used for the other two laser sources except a FS 60º prism was used for dispersing the fundamental and SH beams.

For the polarization dependence measurements, the input polarization angle γ with respect to the plane of incidence was controlled over the range *p*-polarized ($\gamma = 0°$) to *s*-polarized ($\gamma = 90°$) by rotating a half-wave plate and polarizing beam-splitter prior to the sample. A UV-absorbing color filter (Corning 3-69 for example) was placed between the polarization optics and the sample to eliminate the SHG generated by the half-wave plate. A UV polarizing beam-splitter cube was placed in the beam prior to the 60º prism to resolve the *s* and *p* components of the output signal. For all except the polarization dependence studies, the $I_{SHG,pp}$, intensity was measured, where the first and second subscripts refer to the output and input polarizations, respectively.

Results and Analysis

A. Bulk Absorption

Effective extinction spectra of NB perchlorate in water at three different dye concentrations are shown in Figure 2. The series of spectra clearly shows the increasing prominence of a new absorption band on the short wavelength (blue) side of the dye monomer absorption with increasing dye concentration. These blue shifted bands have been previously assigned[35,37,39,45,47] to the formation of H-type dimers.

Following the method of Selwyn and Steinfeld[63] and Rohatgi and Mukhopadyay[64] as applied to OX720 by Gvishi and Reisfeld, [37] the absorption spectra were analyzed to extract values of K_d for the dyes NB, OX720, and CV. The monomer and dimer concentrations can be expressed in terms of the starting monomer concentration M_o and x, the fraction of remaining monomer species, such that $[M] = xM_o$ and $[D] = (1-x)M_o/2$. K_d is then given by:

$$K_d = \frac{[M]^2}{[D]} = \frac{2M_o x^2}{1-x} \qquad (3)$$

The measured absorption spectra were converted to effective extinction spectra ($\varepsilon_{eff}(\lambda) = A(\lambda) / M_o$). A sufficiently dilute solution (<10^{-6} M) with a negligible dimer contribution (as determined by finding no change in the spectral shape upon further dilution) was used as the reference effective extinction spectrum for the monomer, $\varepsilon_M(\lambda)$. The monomer spectrum was then mathematically stripped from a more concentrated extinction spectra to extract an unperturbed dimer spectrum ($\varepsilon_D(\lambda)$). Spectra for additional

concentrations (<10^{-3} M) were then fit as a linear combination of the two limiting cases in terms of x:

$$\varepsilon_{\text{eff}}(\lambda) = x\varepsilon_{\text{M}}(\lambda) + \frac{(1-x)\varepsilon_{\text{D}}(\lambda)}{2} \qquad (4)$$

The results of the analysis for NB are also shown in Figure 2. The peak wavelengths for both the monomer and the dimer bands for all the dyes studied are reported in Table 1. These measurements were also made for the same dye solutions with salt added. Another approach can be used in which a few drops of surfactant are added to the sample to dissociate the aggregates and convert all of the dye into monomer. Our K_d value for OX720 agrees with the value reported by Gvishi and Reinfeld.[37] The change in K_d is similar to what was observed previously with salt.[42] As was discussed above,[35] a quantitative measurement of K_d for the oxazine dyes is complicated by adsorption on the glass surfaces of the cells used. Our measurements show that K_d for OX720 is about 5 times smaller than for NB which is about three times smaller than for CV.

Adding salt (NaCl) to aqueous solutions of dye molecules effects the extent of observed aggregation[36,44]. In the case of the oxazine dyes in this study, the addition of salt leads to a decreased effective association constant as seen in the bulk absorption spectra (not shown). The degree of aggregation (1-x) increases upon the addition of salt (≤ 0.1 M) to the dye solutions such that the (normalized) spectrum $\varepsilon_{\text{eff}}(\lambda)$ / ε_{eff}(max) resembles what is observed for a solution without salt but with an approximately 2-3 times higher dye concentration. The values for samples with salt added, but otherwise identical, were also measured and the K_d results are given in Table 1.

Above a critical salt concentration, aggregation in the dye solution increases to the extent that it becomes visibly cloudy due to the formation of macroscopic sized aggregates. The salt concentration for this to occur was determined for the dye solutions so that the optical studies could be carried out at concentrations low enough to avoid precipitation. Also, comparison of the relative association constants K_d with the amount of salt that induces precipitation for the dyes may address whether K_d is primarily determined by solubility. NB precipitates more readily than the other two dyes. When the salt concentration reaches a certain level (0.1 M), the NB dye solution (3×10^{-4} M) completely converts to macroscopic aggregates within thirty minutes, CV shows initial signs within thirty minutes and completely converts within several hours. OX720 shows only a slight indication of macroscopic aggregation even after a period of several days. The SHG signals were also monitored as a function of salt with similar results. The signal increased and then decreased with salt. The salt concentration at which the signal decreased was 0.012 for NB, and 0.12 M for CV and OX720. NB precipitates first, but K_d is larger for OX720.

The absorption spectra of two other oxazines, oxazine 725 and LD690, were also measured and showed no sign of bulk aggregation in methanol and water, with or without salt, even at the limit of the dye solubility in water.

B. Dye SHG spectra at the interface

Aqueous solutions of NB, OX720, and CV all exhibited measurable SHG signals both with and without salt for laser wavelengths near 600 nm. For CV without salt, the signal was close to the detection limit. Surface absorption spectra for these three dyes with salt were collected with the SHG technique using both the nanosecond and picosecond laser systems described in the experimental section. The SHG signals were recorded as a function of incident laser wavelength and the results are plotted in Figure 3. The linear bulk absorption spectrum is also shown for reference at both the fundamental (ω) and two photon (2ω) wavelengths. The relative SHG amplitude, $E_{\mathrm{SHG}} \propto \sqrt{I_{\mathrm{SHG}}}$, is plotted rather than the signal intensity to compare directly with the wavelength dependence of $\chi^{(2)}$ (as depicted in Equation 2). The SHG spectra exhibit only a single absorption feature which is attributed to the aggregate. The absorption feature is red shifted from the aggregate in the bulk linear spectra. The SHG spectra were fit to a Gaussian profile and the peak center frequencies and widths are reported in Table 1.

C. Effects of bulk solution composition on the interface from SHG measurements.

The dependence of the SHG signal on the bulk concentration of the dye was measured for NB and OX720 using the ultrafast system described in the experimental section. CV was not measured because the SHG signal was near the detection limit and barely distinguishable from the bulk (two photon) fluorescence induced by the laser. The

concentration dependence of the SHG signal intensity for each sample was then fit to a Langmuir isotherm in a similar manner to the methods of Das et al.[43] and Haslam et al.[51] The functional form of the isotherm is given as:[65,66]

$$\theta = \frac{SkD}{(1+kD)} \tag{5}$$

where θ represents the surface coverage in terms of a monolayer, S is a scaling factor, D is the bulk concentration of the observed species, and k is the surface adsorption equilibrium constant. Since $I_{\mathrm{SHG}} \propto D^2$, The experimental data is fit using,

$$I_{\mathrm{SHG}} = \theta^2 \tag{6}$$

As will be presented in the discussion, the SHG signal arises only from the dye aggregate and the appropriate concentration to use is therefore the dye aggregate concentration [D] and not the monomer. The dimer concentration, [D], is determined for each initial monomer concentration using the bulk K_{d} value determined in the previous sub-section. A nonlinear fitting routine was used to fit the experimental data to the isotherm model and extract a value for k. The adsorption free energy is given by, $\Delta G_{\mathrm{ad}} = -\mathrm{R}T \ln K$ where $K = 55.5 \times k$.[43,50,51] The values determined for ΔG_{ad} are reported in Table 2. The NB isotherm is shown in Figure 4a. The inset in Figure 4a shows the isotherm plotted against the uncorrected bulk monomer concentration for comparison.

SHG studies were also carried out for modified or similar dye solutions. This includes adding components as well as solutions composed of other oxazine dyes and other solvents. The addition of the surfactant Triton X-100 had the most dramatic effect on the SHG signal intensity, which was reduced to below our detection limit. Similar results were observed

using polystyrene sulfonic acid. The dimers are almost completely eliminated in the surfactant-modified dye solutions. This is evident from the linear spectra in which the dimer bands disappear and a single absorption band near that for the monomer remains with higher absorbance. The bands are red-shifted (by as much as 20 nm) relative to the monomer peaks for the solutions without surfactant. The correlation between the surfactant effect on the SHG signal intensity and the change in the bulk absorbance spectrum suggests that the SHG signal is due to the aggregate species alone. This conclusion is supported by our result that no SHG signal was observed for aqueous solutions of oxazine 725 or LD690 nor for NB, CV or OX720 in methanol or ethanol solutions, even when salt was added.

The dye concentration dependence of the SHG signal for NB, OX720, and CV was also measured in the presence of salt. The experimental data was fit to an isotherm model and the ΔG_{ad} values for the salted samples are also reported in Table 2. As was noted in the determination of the bulk K_d values, the addition of salt to the bulk effectively increases the value of K_d by a factor of 2-3. The modified K_d were used to calculate the dimer concentrations. The salted NB isotherm is shown in Figure 4b. Unlike the isotherms for the unsalted dye solutions, the SHG signal does not increase monotonically to a limiting value. Instead, the SHG signal rises with increasing dye concentration to a maximum value and then decreases. A similar effect was observed by Sarkar et al.[50] for the addition of the water-soluble surfactant cetyltrimethylammonium bromide, CTAB, to aqueous solutions of PNP. In the case of CTAB, the decrease was attributed to a decrease in surface ordering due to the increased surface coverage of PNP, or from the raising of ΔG_{ad} for the sample upon the addition of CTAB.

D. SHG Polarization Dependence and Molecular Orientation

The polarization dependence of the SHG signal intensity, I_{SHG}, can be used to characterize the orientation and relative hyperpolarizabilities of a species at the surface.[1,10,13] Measuring the polarization dependence helps to discriminate whether changes in I_{SHG} as a function of the bulk solution composition result from changes in the concentration, orientation or nonlinear optical properties. The observed signals depend on the angle of incidence, θ, and the input laser polarization angle, γ, where $\gamma = 0°$ corresponds to *p*-polarization. For a molecular orientation that is isotropic about the surface normal, as expected for an air/water interface system, there are five nonzero second-order susceptibilities, χ_{ZZZ}, χ_{ZXX}, χ_{XXZ}, χ_{ZZX}, and χ_{ZXZ}, where χ_{ZZZ}, χ_{ZXX}, and χ_{XXZ} are unique. The (2) superscripts indicating second-order terms of the various tensors have been dropped at this point in the manuscript for clarity. The *s*-polarized ($I_{SHG,s}$) and *p*-polarized ($I_{SHG,p}$) output SHG intensity can be expressed in terms of the input laser intensity I_ω as (the SHG subscript will be dropped from this point for clarity):

$$I_s \propto \left| a_1 \sin 2\gamma \, \chi_{XXZ} \right|^2 (I_\omega)^2 \qquad (7a)$$

$$I_p \propto \left| (a_2 \, \chi_{XXZ} + a_3 \, \chi_{ZXX} + a_4 \, \chi_{ZZZ}) \cos^2 \gamma + a_5 \chi_{ZXX} \sin^2 \gamma \right|^2 (I_\omega)^2 \qquad (7b)$$

The coefficients a_1 - a_5 represent the electric field components at the surface.[10,53,67,68] They are the products of the linear and nonlinear Fresnel factors and as well as the geometric factors and include the dielectric constants for the bulk and interfacial phases. The susceptibilities and any derived quantities, such as orientational parameters, are actually

effective ones if the optical constants are not determined, as in this case.[53,68] Since we are unable to obtain linear surface spectra for our samples, for the present analysis, the interfacial dielectric constant is assumed to be close to an average of the bulk values ($\varepsilon(\omega) = \varepsilon(2\omega) = 1.2$), and the parameters obtained are to be considered effective values.

The SHG polarization dependence was measured for all three oxazine dyes in water both with and without salt. The results for OX720 (6×10^{-4} M) with 0.1 M NaCl and for NB (3×10^{-4} M) are shown in Figure 5. The data were fit to the form of Equation 7 to derive the relative χ's. In many cases only I_{pp}, I_{ps} and $I_{s,45}$ were measured. In cases where $I_{s,45}$ was detected, I_{sp} and I_{ss} were also measured to confirm that the signals were due to SHG. The results are shown in Table 3. The polarization anisotropy measurements for all the solutions exhibited the same qualitative behavior: $I_{ps} \approx 1.5 \times I_{pp}$ and I_p (all γ) >> $I_{s,45}$. The *s*-polarized output was so weak that in several cases it was not detectable. In these cases, a value of $I_p = 20\ I_{s,45}$ was assumed. The results presented demonstrate that increasing the concentration of the dye or adding salt to the solutions is not accompanied by any large changes in the polarization dependence even thought the I_{SHG} magnitude does increase substantially. This can be seen more clearly by analyzing the data to obtain microscopic molecular parameters.

The macroscopic susceptibilities are related to the molecular hyperpolarizabilities (β) by the transform function $T_{IJKijk}(\phi,\theta,\delta)$ such that[10]

$$\chi_{IJK} = N_S \sum \left\langle T_{IJKijk}(\theta,\phi,\delta) \right\rangle \beta_{ijk} \qquad (8)$$

where $T_{IJKijk}(\phi,\theta,\delta)$ depends on the Euler angles for the molecular orientation at the surface. The angle θ is the angle between the molecular *z*-axis (the short, in-plane axis for the oxazine

dyes) and the surface normal, δ is rotation about the *z*-axis, and ϕ is the azimuthal angle, which for our case is assumed to be a random, isotropic distribution. Two factors (in addition to the assumptions for the dielectric constants) that strongly affect the derived microscopic parameters are the following: 1) how many and which β's are significant, and; 2) the orientational distribution function. In principle, all three unique, non-zero β's can contribute significantly, but the analysis is simplified if this number can be reduced to one or two. It has been shown that when one β is dominant it is reflected in the relative values of the χ's.[69] If χ_{ZZZ} is dominant, then $\chi_{ZXX} = \chi_{XXZ}$, and if χ_{XXZ} (or χ_{ZXX}) is dominant, then $\chi_{ZZZ} = -2\ \chi_{ZXX}$ (or $\chi_{ZZZ} = -2\ \chi_{XXZ}$). Neither of these conditions is satisfied by our results (within the range of reasonable values for ε), so two β's are assumed to be significant. It would be preferable to have *ab initio* calculations to guide the choice of β's, but we will follow the precedent established in previous studies of aromatic dye molecules that the relevant hyperpolarizabilities are β_{ZXX} and β_{XZZ}. The basis for this is that the most likely transition moments (S_0-S_1 and S_0-S_2) are expected to lie in the plane of the molecule. β_{ZXX} and β_{XZZ} were assumed to be dominant in earlier studies for nominally planar aromatic dye molecules, such as for eosin B,[19,23] rhodamine 110,[60] MG,[54] R6G.[55] Corn and coworkers carried out calculations of the hyperpolarizabilities in their studies of methylene blue[52,53] and found these to be the dominant ones. The dominant β's for the dimer are also assumed to be the same as for the monomer. This does not seem unreasonable for sandwich-type (or H-type aggregates) dimers for which the transition moments are aligned.

Equation 8 can be used to derive molecular parameters for the orientational distribution and the relative β's, depending upon assumptions for the former. In the present

study, where β_{ZXX} and β_{XXZ} are dominant, the ratio of these hyperpolarizabilities, β_r, is given by

$$\beta_r = \frac{\beta_{XXZ}}{\beta_{ZXX}} = \frac{\chi_{ZZZ} + 2\chi_{XXZ}}{\chi_{ZZZ} + 2\chi_{ZXX}} \tag{9}$$

This ratio indicates whether these hyperpolarizabilities are both significant. The results presented in Table 3, for all of which $0.19 < \beta_r < 0.42$, indicate that both β_{ZXX} and β_{XXZ} contribute to the signal for the solutions investigated. The orientation parameter, $D(\theta)$, which can also be obtained from Equation 8, is given by

$$D(\theta) = \frac{<\cos^3\theta>}{<\cos\theta>} = \frac{Y\chi_{ZZZ} + 4\chi_{ZXX} + 2\chi_{XXZ}}{3\chi_{ZZZ} + 4\chi_{ZXX} + 2\chi_{XXZ}} \tag{10}$$

where the brackets denote the distribution average. The general solution for $D(\theta)$ is expressed in terms of the distribution of the angle δ by the parameter $Y = 3 - \left\langle \cos^2 \delta \right\rangle^{-1}$. A random distribution in δ is sometimes assumed in the literature and this assumption yields the same expression for D as $\delta = 45°$ (for which $Y = 1$). The angle θ obtained from D depends on the distribution assumed for this angle. The values for a narrow distribution for $\delta = 0°$ and for $\delta = 45°$ (which is the same result as for a random distribution) are presented in Table 3.

Discussion

Several types of SHG studies were carried out for three of the oxazine dyes at the air/water interface. The interpretation of the results is that the surface SHG signals measured are due almost entirely due to H-aggregate dimers at the interface. The same conclusion was reached by Levinger et al.[44] to explain the SHG spectra they measured for the water-soluble dye IR125 at the air/water interface. For the present work, the case is strengthened by results of additional SHG measurements. The SHG spectra appear to be due to a single species; they are narrower and slightly red-shifted compared to aggregates observed in the bulk. The SHG signal and the degree of aggregation in the bulk depend on the solution composition in the same way. Both the SHG signal intensity and the value of K_d increase upon adding salt and the opposite is observed when surfactant is introduced. Also, no SHG signal was observed for the oxazines with only three aromatic rings (OX725 and LD690) that do not observably aggregate in the bulk. The SHG polarization dependence does not depend strongly on the dye concentration nor on the presence of salt, suggesting that the signals originate from the same species regardless of solution composition. The following remarks are intended to develop the interpretation that the results can be explained in terms of the signals arising solely from H-aggregates and to demonstrate consistency with previous results and the conclusions regarding air/water interfaces.

As described in previous bulk absorption studies, CV, NB, and OX720 readily form H-aggregates in aqueous solutions. Bulk solution absorption measurements are reported, and the corresponding K_d values obtained are listed in Table 1. They are in agreement with previous studies. Adding salt ($\leq$ 0.1 M) increases K_d by a factor of 2-3 for the dyes. OX725

and LD690 do not aggregate to nearly the same extent. CV, NB, and OX720 have a fourth aromatic ring in the backbone structure that is missing in the other two oxazines. The added hydrophobicity from the fourth ring in NB, CV, and OX720 most likely accounts for their stronger tendency to form dimers. The relative K_d values correlate with the expected hydrophobicities of the dyes: OX720 > NB > CV. Upon examining the salt effect on the dye solutions, we found that NB precipitates at a lower salt concentration but OX720 has a higher K_d. The trend for precipitation is opposite to that for aggregation, indicating that the observed aggregation is not simply due to a reduction of dye solubility in salted versus unsalted solutions.

In considering whether to expect more dimer or monomer for the oxazines at the surface (relative to their abundances in the bulk) it is useful to point out that previous studies of adsorbate properties suggest that the air/water interface is less polar than the bulk aqueous phase. This is supported by concentration dependence measurements of the SHG signal intensity which yield adsorption free energies, ΔG_{ad}, for various molecules. Phenols are probably the most extensively studied soluble species at aqueous interfaces. ΔG_{ad} for PNP is about -6 kcal/mol, [17,43,50] whereas for the less polar *p*-heptylphenol, ΔG_{ad} is -9.3 kcal/mol.[17] Similarly, pK_a values determined for surface adsorbates are higher for acids and lower for bases, both suggesting that the neutral form is preferred at the interface.[17-20] These results indicate that the polarity of the surface layer is lower than that of the bulk solution. Studies in which solvent shifts were measured for solvatochromatic dyes at air/liquid and liquid/liquid interfaces, including the air/water interface, by Wang et al. also directly support a surface polarity that is lower than the bulk.[15,16] The observed shifts and the corresponding interface polarity are approximately equal to the average value of the polarities for the two

homogeneous phases that comprise the interface. Oxazine dyes are water soluable and therefore the effects of additional equilibria must also be considered. In addition to the equilibrium in the bulk between dye monomer and dimer, the individual adsorption equilibrium for the two species and the surface aggregation equilibrium must be considered. In this study, the resulting SHG signal intensity appears to derive almost exclusively from the aggregate, which implies relative values for constants of the various coupled equilibria must exist. Dimer adsorption is favored over monomer adsorption ($\Delta G_{ad,mono} > \Delta G_{ad,dimer}$). Also the surface aggregation equilibrium must favor the dimer more strongly than in the bulk ($K_{d,surf} < K_{d,bulk}$). Additionally, the oxazine dimers are less polar than the monomers and therefore they should be the predominant species at the surface for the dye solutions.

The bulk composition results from this study include measurements of the SHG signal intensity as function of dye concentration as well as for the addition of other constituents to the bulk solution. The SHG signal intensity and bulk aggregation correlate with solution composition changes and this provides evidence that the SHG signal is due to dimers at the interface. A complication is that for some compositional changes, increased monomer adsorption would also be expected. The surfactant Triton-X is very effective at dissociating the dimers and producing a solution which consists almost entirely of dye monomer. The observed SHG intensity is eliminated by the surfactant and this implies that dimers are responsible for the SHG. However, the surfactant may simply cover the surface and crowd out all other species. In this case, the observation would not yield any information regarding the nature of the surface species. We were also unable to detect SHG signal from aqueous solutions of the other oxazine dyes (OX725 and LD690) or from methanol and ethanol solutions of any oxazine. From absorbance measurements, few if any dimers are

formed under these conditions. SHG is not detected for the oxazines under circumstances in which SHG should be observed if the signal were due to the monomer. Once again, these observation are similar to those reported by Levinger et al.[44] who detected little or no SHG from IR125 in methanol or acetone which provide a poor aggregation environment.

Our concentration dependence results yield fairly large magnitude values for ΔG_{ad} (-9.7 to -14.6 kcal/mol). An isotherm model, using the dimer concentration [D] as the concentration, was used to calculate the value of ΔG_{ad}. The dimer concentration was determined using Equation 3 from the initial dye concentration [M_o] and K_d. The ΔG_{ad} values for NB and OX720 are –9.7 and –10.4 kcal/mol, respectively, and these are slightly more negative than the value reported for *p*-heptylphenol.[17] Adding salt (0.01 M for NB and 0.1 M for OX720 and CV) decreases the ΔG_{ad} for NB and OX720 by 4.4 and 4.2 kcal/mol, respectively. The value for CV with salt is considerably higher (-9.7 kcal/mol) than for the other two dyes with salt. This may be due to the somewhat lower hydrophobicity for CV which would reduce the driving force for the solution to push the dimer to the surface. Salt increases the SHG signal intensity and it also promotes aggregation in the bulk, probably for the same reason. But as reported by Das et al.,[43] even for monomeric organic species, such as PNP, salt can reduce ΔG_{ad} values. Correlating the salt effect for bulk dimer and surface SHG is therefore not a clear demonstration that dimers at the surface are causing SHG. The isotherms for the dyes alone increase monotonically. The samples with salt increase to a maximum value and then decrease 30-50% of the maximum value upon further addition of dye or salt. This effect was observed both when salt was added while maintaining a constant dye concentration and while adding dye to a constant salt concentration. The decrease at higher concentrations may be due to the formation of higher aggregates that do not generate

SH at these wavelengths as efficiently as the dimer. Increasing the salt or dye concentrations much beyond the point where a decrease in the SHG signal is observed resulted in formation of macroscopic particles of precipitate.[70]

The salt effect on the oxazine SHG signals is quite dramatic. A strong increase is observed for low salt concentrations. The largest signal enhancement is observed for a concentration of about 0.1 M for CV and OX720 and 0.01 M for NB. This is a much lower concentration than those used in previous studies investigating salt effects on K_d (1.8 M),[42] and surface adsorption (3 M).[43] Adding salt to the oxazine solutions increases the observed SHG signal to a greater extent than it increases the dimer concentration in the bulk. In the latter case, K_d increases by about a factor of 2-3.[71] The SHG signal increases by as much as a factor of 30 (for CV) and by more if the dye concentration is low (relative to that for the maximum SHG without salt – See Figure 4). If this effect were solely due to a change in N_s, the surface dimer concentration, then it would imply that N_s is higher by a factor 5.5, as $I_{SHG} \propto N_s^2$. Since there is no strong observed concentration or salt effect on the orientation based on the polarization dependence studies, it is not unreasonable that all the changes in the SHG signal intensity associated with the changes in the solution composition are in fact due to changes in N_s.[72]

The results for the SHG spectra and polarization dependence indicate that the signals are due to a single species. There have been few previous studies that include reports of SHG electronic spectra for soluble adsorbates at the air/water interface. Those studies that have been made include the work of Wang et al.[15,16] for solvachromatic dyes and by Levinger et al. for IR125,[44] both of which have been described above. In the latter case, the SHG spectra clearly indicated that aggregates were responsible for the SHG signals. The SHG

spectra closely resembled the bulk solution spectra of the aggregate, which were substantially different than the monomer spectra.

In the present work, it is not as straightforward to ascribe the SHG signal to the monomer or dimer based on the spectra alone. This is because the SHG signal bands are slightly red-shifted as compared to the dimer spectrum in solution. If the polarity is lower at the interface, one might expect the surface bands to be blue-shifted instead. The SHG spectra measured for the oxazines, shown in Figure 3 for solutions with salt, indicate that SHG arises from a single species. In each case, the band consists of a single peak that falls between those for the monomer and the dimer in solution. Comparison shows that the SHG bands are considerably narrower (about 80 nm FWHM) than the absorption spectra for the bulk solution also shown in Figure 3.[73] The SHG spectra appear to be primarily due to a resonance with the incident beam near the first electronic absorption of the dyes. There is no increased signal on the short wavelength edge of the bands that might arise from a resonance at the second harmonic frequency. The relevant portion of the dye UV absorption spectrum is also plotted in Figure 3. In an early SHG study of NB on silica, Marowsky et al.[74] found a marked increase in the SHG signal as compared to R6G due to a resonance at both the fundamental and the second-harmonic frequencies. If the difference between the present study and that of Marowsky et al.[74] does not simply arise from the differing substrates (water versus silica), another explanation could be that our signals are from dimers and the NB on silica SH signals are from the monomer. This might explain why the susceptibility is dominated by the first electronic transition (with ω) in our case and there is a significant contribution from the higher transition in the UV (with 2ω) in the results by Marowsky et al.[74] The oxazine SHG band centers measured were in between those in the solution for

the monomer and dimer band positions. For NB, the band is very close to that for the solution dimer, for OX720 it is nearly halfway between the two and for CV it is closer to the monomer. For reasons outlined above, if the air/water interface is less polar than the bulk and if the SHG bands are due to dimers, we would expect them to occur to the blue of the solution dimer band. Other factors may account for the apparent red-shift. The dimer structures may be slightly different at the interface than in the bulk. If the separation of the dye units within the dimer were a little longer, for example, this would reduce the aggregate induced blue shift relative to the monomer.[75] It could be that the environment around the adsorbates experiences a higher polarity due to intermolecular interactions among the adsorbates. This effect has been reported in several studies especially for rhodamines on silica, albeit for dyes adsorbed on solid substrates rather than for aqueous interfaces. Kemnitz et al.[76] and then Peterson and Harris[60] observed this as red shift in absorption band for rhodamine B on silica as a function of coverage. More recent examples can also be found in the work by Leach and coworkers on MG and R6G,[54,55] also on silica.[77]

One of the major results from the polarization studies is the measurement of the orientation of the aggregates with respect to the surface and that the orientation is not strongly affected by changes in solution composition. As shown in Table 3, for all three dyes both with and without salt, the $I_{s,45}$ signals (for $\gamma = 45°$) are much lower than for I_p (all γ) and I_{pp}/I_{ps} is 0.45-0.80. I_s was too small for us to detect in half of the samples (for OX720 and CV without salt and CV with salt). I_s is small in all cases, whether we were able to detect it or not, and the *p*-out ratio, I_{pp}/I_{ps}, is the same with and without salt for each dye within our uncertainty (which is about 20% for the intensity ratios); the difference between solutions with and without salt is about 13% for CV and OX720 and 22% for NB. The *p*-out ratio was

also found to be the same for concentrations from 10^{-6}-10^{-4} M for OX720 with salt. The weak polarization dependence indicates that the SHG intensity originates from one species, the dimer, for each dye regardless of solution composition and that the associated changes in the SHG signals are due to surface coverage rather than orientation changes.[78]

There are previous reports of SHG studies that have found that the adsorbate orientation was not affected by the solution composition or surface coverage. While investigating the effects of salts on surface coverage at the air/water interface for PNP, Das et al.[43,50] measured the polarization dependence and found that the orientation was unaffected. Similarly, Frey and coworkers[51] characterized the effect of TBP on the PNP coverage at the dodecane/water interface and determined that no orientation changes occurred. For submonolayer coverages of Rhodamine 110 (R110) on silica, Morganthaler and Meech[60] concluded that the orientation did not change. Leach and coworkers[54] investigated the R6G system and their results indicate a change in the polarization dependence or orientation only for coverages exceeding a monolayer.

The relative susceptibilities, χ, were determined and used to derive the molecular parameters θ and β_r as described above. The χ's indicate that the analysis should include at least two hyperpolarizabilities and we have taken β_{ZXX} and β_{XXZ} to be dominant. This is consistent with the dye structures and follows the precedent established for planar aromatic dyes for SHG involving a resonance with a transition from the ground to the first electronic state.[52-54,56,59] Using a single β is more often appropriate for probe wavelengths far from resonance. The results are presented in Table 3. There is about 30% uncertainty in the assumed values for the interface dielectric constant and this propagates to $\pm$ 3° in the values

for θ. The calculations were also performed for the samples in which I_s was not detected for purposes of illustration. The values determined for β_r demonstrate that both susceptibilities contribute significantly. The orientation parameters are close to 0.90 for all the samples. The orientation angles θ were calculated using Equation 10 assuming the distribution with respect to the *x*-axis is either narrow about $\delta = 0°$ or is random with respect to δ. The values for θ are 12-26°. There is no difference in θ within our uncertainty for each dye, with or without salt, demonstrating that the dimer orientation is not strongly affected by the presence of salt. There does appear to be a slight difference among the dyes, in which the alignment of the *x*-axis with the surface normal is highest for NB and lowest for CV. The results indicate that for all the dyes the *x*-axis, the short, in-plane axis, is more perpendicular than parallel to the surface. All three dye aggregates have similar orientation angles. This is not surprising since they have very similar chemical structures, differing only in the ordering of the substituents on the two terminal amine groups and an addition methyl group for OX720. At the same time, there are appreciable differences in the bulk K_d's, OX720 > NB > CV, and for the adsorption free energies, CV > NB ≈ OX720. The angles obtained for θ for the oxazine dye dimers at the air/water interface are slightly lower than those (30-40°) measured for other polyaromatic dyes on water.[23,59] It is quite possible that the oxazine dimers are situated with a range of angles, that the distribution has an appreciable width. It is not possible to determine the width and mean of the distribution with the SHG polarization results alone. One way to accomplish this is to combine the SHG results with another orientation sensitive measurement, such as linear polarization spectroscopy.[62] If the distribution is considered to be a Gaussian in θ, $G(\theta)$, then

$$D(\theta) = \frac{\left\langle G(\theta)\cos^3(\theta)\right\rangle}{\left\langle G(\theta)\cos(\theta)\right\rangle} \tag{11}$$

yields solutions for *D* in which the mean angle decreases as the width is increased. Therefore, to the extent the assumed distribution affects θ, which we find to be small (less than 1°), our results based on a narrow distribution represent an upper limit if the distribution is Gaussian.

An alternative method for analyzing the orientation angle was presented by Peterson and Harris[60] and applied for two hyperpolarizabilities by Higgins et al.[53] If the constraints on δ are removed, an expression based on Equation 8 can be developed for the molecular orientation with respect to the long, in-plane *x*-axis, ξ:

$$\cos^2(\xi) = \cos^2(\delta)\sin^2(\theta) = \frac{(1+2\boldsymbol{\beta}_r)^{-1}}{\boldsymbol{\chi}_{ZZZ}+2\boldsymbol{\chi}_{ZXX}} \tag{12}$$

The derived angles for ξ are listed in Table 3. They are all near 75º, which indicates that the dimers have their long axes almost parallel to the surface. The result for ξ for each solution mathematically corresponds to a family of solutions in terms of δ and θ as shown by Kikteva et al.[54] for their results of R6G on silica. The values of θ which can satisfy Equation 12 run from some minimum value (~15º in this study) to $\theta = 90º$. The minimum in θ occurs at $\delta = 0º$, for which $\theta = \text{asin}(\cos\xi)$. For the case of $\theta = 90º$, $\delta = \xi$. Kikteva et al.[54] demonstrated the useful check that the value of θ determined for $\delta = 0º$ should correspond to the one obtained from the orientation parameter. The angles for ξ are somewhat higher than those reported for MB dimers[53] on silica, $\xi \approx 60º$.

Conclusions

Steady-state SHG studies have been carried out for oxazine dyes at the air/water interface. The dyes readily aggregate in the bulk and the combined evidence from various types of SHG measurements indicate that the SHG arises from dimers. The SHG spectra and and polarization dependence results indicate that a predominant surface species that is not strongly affected by the composition of the solution is the source. The signals depend on the solution composition in a manner that reflects aggregation in the bulk. Levinger et al.[44] also found that the SHG signals they observed for a soluble dye in liquid water originated from aggregates. It has been shown in previous studies of adsorbates at the air/water interface that it is less polar than bulk water and that less polar molecules adsorb preferentially. This is consistent with our conclusions that the less polar oxazine dimers are preferred at the interface over the monomeric species. Furthermore, our results provide further evidence that hydrophobicity induces adsorption at the air/water interface. The higher degree of aggregation at the air/water interface suggests that the enhanced aggregation observed for the oxazine at aqueous/solid interfaces[28,46-49] may have a contribution from the liquid phase as well as the solid. The high propensity for aggregation at the air/water interfaces also means that organic species involved in marine surface chemistry are more likely to be affected by this process. Further studies on this system, including ultrafast measurements to characterize the excited state dynamics, will be published shortly.

Acknowledgments

This work was supported by the Office of Naval Research through the Naval Research Laboratory. This work was performed while DAS held a Naval Research Laboratory - National Research Council Research Associateship. We thank Jim Fleming and Brad Williams for the use of their picosecond laser system and Steve McIlvaney for the use of his nanosecond laser system. We also acknowledge Andy Baronavski for many helpful discussions.

References

1. Heinz, T. F.; Chen, C. K.; Richard, D.; Shen, Y. R. *Phys. Rev. Lett.* 1982, *48*, 478-481.

2. Heinz, T. F.; Tom, H. W. K.; Shen, Y.R. *Phys. Rev. A* 1983, *28*, 1883-1885.

3. Hunt, J. H.; Guyot-Sionnest, P.; Shen, Y. R.; *Chem. Phys. Lett.* 1987, *133*, 189-192. Guyot-Sionnest, P.; Superfine, R.; Hunt, J. H.; Shen, Y. R., *Chem. Phys. Lett.* 1988, *144*, 1-5.

4. Goh, M. C.; Hicks, J. M.; Kemnitz, K.; Pinto, G. R.; Bhattacharyya, K.; Heinz, T. F.; Eisenthal, K. B.; *J. Phys. Chem.* 1988, *92*, 5074-5075.

5. Hicks, J. M.; Kemnitz, K.; Eisenthal, K. B. *J. Phys. Chem.* 1986, *90*, 560-562.

6. Shen, Y. R. *Ann. Rev. Phys. Chem.* 1989, *40*, 327-350. Shen, Y. R. *Ann. Rev. Mater. Sci.* 1986, *16*, 69-86. Shen, Y.R. *Surf. Sci.* 1994, *300*, 551-562 and references 5 and 6 therein.

7. Eisenthal, K. B. *J. Phys. Chem.* 1996, *100*, 12997-13006.

8. Eisensthal, K. B. *Ann. Rev. Phys. Chem.* 1992, *43*, 627-661.

9. Eisensthal, K. B. *Chem. Rev.* 1996, *96*, 1343-1360.

10. Heinz, T.F. *Nonlinear Surface Electromagnetic Phenomena*, edited by Ponath, H.-E.; Stegeman, G. I.; North Holland: Dordrecht, 1991.

11. Shultz, M. J.; Schnitzer, C.; Simonelli, D.; Baldelli, S. *Int. Reviews in Physical Chemistry* 2000, *19*, 123-153.

12. Mizrahi, V.; Sipe, J. E. *J. Opt. Soc. Amer. B* 1988, 5, 660-667.

13. Corn, R. M.; Higgins, D. A. *Chem. Rev.* 1994, *1994*, 107-125.

14. Dick, B.; Hochstrasser, R. M. *Chem. Phys.* 1984, *91*, 1-11.

15. Wang, H. F.; Borguet, E.; Eisenthal, K. B. *J. Phys. Chem. B* 1998, *102*, 4927-4932.

16. Wang, H. F.; Borguet, E.; Eisenthal, K. B. *J. Phys. Chem. A* 1997, *101*, 713-718.

17. Bhattacharyya, K.; Castro, A.; Sitzmann, E. V.; Eisenthal, K. B. *J. Chem. Phys.* 1988, *89*, 3376-3377.

18. Zhao, X.; Subrahmanyan, S.; Eisenthal, K. B. *Chem. Phys. Lett.* 1990, *171*, 558-562.

19. Tamburello-Luca, A. A.; Hébert, Ph.; Antoine, R.; Brevet, P. F.; Girault, H. H. *Langmuir* 1997, *13*, 4428-4434.

20. Zhao, X.; Ong, S.; Wang, H.; Eisenthal, K. B. *Chem. Phys. Lett.* 1993, *214*, 203-207.

21. Shi, X.; Bourget, E.; Tarnovsky, A. N.; Eisenthal, K. B. *Chem. Phys.* 1996, *205*, 167-178.

22. Castro, A.; Sitzmann, E. V.; Zhang, D.; Eisenthal, K. B. *J. Phys. Chem.* 1991, *95*, 6752-6753.

23. Antoine, R.; Tamburello-Luca, A. A.; Hébert, Ph.; Brevet, P. F.; Girault, H. H. *Chem. Phys. Lett.* 1998, *288*, 138-146.

24. Bourdon, J. *J. Phys. Chem.* 1965, *69*, 705-713.

25. Herz, A.H. “Adsorption of sensitizing dyes to silver halides,” in *The Theory of the Photographic Process, 4th ed.*, edited by James, T. H.; MacMillan: New York, 1977; pages 235 – 249.

26. Hagfeldt, A.; Grätzel, M. *Chem. Rev.* 1995, *95*, 49-68.

27. Henglein, A. *Chem. Rev.* 1989, *89*, 1861-1873.

28. Kamat, P. V. *Chem. Rev.* 1993, *93*, 267-300.

29. Hoffmann, M. R.; Martin, S. T.; Choi, W.; Bahnemann, D.W. *Chem. Rev.* 1995, *95*, 69-96.

30. Rabinowitch, E.; Epstein, L. F. *J. Am. Chem. Soc.* 1941, *63*, 69-78.

31. McRae, E. G.; Kasha, M. *J. Chem. Phys.* 1958, *28*, 721-722.

32. McRae, E. G.; Kasha, M. *Physical Processes in Radiation Biology*, edited by Augenstein, L.; Mason, R.; Rosenberg, B.; Academic Press: New York, 1964; page 23.

33. Kasha, M.; Rawls, H. R.; El-Bayoumi, M. A. *Pure Appl. Chem.* 1965, *11*, 371-392.

34. Anfinrud, P.; Crackel, R. L.; Struve, W. S.; *J. Phys. Chem.* 1984, *88*, 5873-5882.

35. Herkstroeter, W. G.; Martic, P. A.; Farid, S. *J. Amer. Chem. Soc.* 1990, *112*, 3583-3589.

36. Isak, S. J.; Eyring, E. M. *J. Phys. Chem.* 1992, 96, 1738-1742.

37. Gvishi, R.; Reisfeld, R. *Chem. Phys. Lett.* 1989, *156*, 181-186.

38. Oxazine 170 is the Kodak brand name. Oxazine 720 is the corresponding Exciton brand name. Alternative names for the dyes will be indicated in parentheses to reduce confusion.

39. Morozova, Y. P.; Zhigalova, E. B. *Russ. J. Phys. Chem.* 1982, *56*, 1526-1528.

40. The approach has been used to investigate the effects of dimers in dye solutions by converting all the dye to monomers. The method was used by Anfinrud et al.[34] to study the fluorescence quantum yield in aqueous solutions of CV and it is used in the present study as a way to measure the equilibrium constant.

41. Valdes-Aguilera, O.; Neckers, D. C. *Acc. Chem. Res.* 1989, *22*, 171-177. Burdett, B. C. *Aggregation Processes in Solution*, edited by Wyn-Jones, E.; Gormally, J.; Elsevier: New York, 1983; page 241. Craven, B. R.; Griffith, B. R.; Kennedy, J.G. *Aust. Chem.* 1975, *28*, 1971-1975. Herz, A.H. *Adv. Colloid Interface Sci.* 1977, *8*, 237-298.

42. Nüesch, F.; Grätzel, M. *Chem. Phys.* 1995, *193*, 1-17.

43. Das, K.; Sarkar, N.; Das, S.; Datta, A.; Nath, D.; Bhattacharyya, K. *J. Chem. Soc. Faraday Trans.* 1996, *92*, 4993-4996.

44. Levinger, N. E.; Kung, K. Y.; Luther, B. M.; Willard, D. M. "Absorption spectroscopy at liquid interfaces by resonant surface second harmonic generation," in *Laser Techniques for Surface Science II*, edited by Hicks, J. M.; Ho, W.; Dai, H.-L. *Proc. SPIE* 1995, *2547*, 400-410.

45. Liu, D.; Fessenden, R. W.; Hug, G. L.; Kamat, P.V. *J. Phys. Chem. B* 1997, *101*, 2583-2590.

46. Liu, D.; Kamat, P.V. *Langmuir* 1996, *12*, 2190-2195.

47. Martini, I.; Hartland, G. V.; Kamat, P. V. *J. Phys. Chem. B* 1997, *101*, 4826-4930.

48. Liu, D.; Kamat, P. V. *J. Chem. Phys.* 1996, *105*, 965-970.

49. Nasr, C.; Hotchandani, S. *Chem. Mater.* 2000, *12*, 1529-1535.

50. Sarkar, N.; Das, K.; Das, S.; Nath, D.; Bhattacharyya, K. *J. Chem. Soc. Faraday Trans.* 1995, *91*, 1769-1773.

51. Haslam, S.; Croucher, S. G.; Hickman, C. G.; Frey, J.G. *Phys. Chem. Chem. Phys.* 2000, *2*, 3235-3245.

52. Campbell, D. J.; Higgins, D. A.; Corn, R. M. *J. Phys. Chem.* 1990, *94*, 3681-3689.

53. Higgins, D. A.; Byerly, S. K.; Abrams, M. B.; Corn, R.M. *J. Phys. Chem.* 1991, *95*, 6984-6990.

54. Kikteva, T.; Star, D.; Zhao, Z.; Baisley, T. L.; Leach, G. W. *J. Phys. Chem. B* 1999, *103*, 1124-1133.

55. Kikteva, T.; Star, D.; Leach, G. W. *J. Phys. Chem. B* 2000, *104*, 2860-2867.

56. Morgenthaler, M. J. E.; Meech, S. R. *J. Phys. Chem.* 1996, *100*, 3323-3329.

57. Zimdars, D.; Dadap, J. I.; Eisenthal, K. B.; Heinz, T. M. *Chem. Phys. Lett.* 1999, *301*, 112-120.

58. Zimdars, D.; Eisenthal, K. B. *J. Phys. Chem. A* 1999, *103*, 10567-10570.

59. Slyadneva, O. N.; Slyadnev, M. N.; Tsukanova, V. M.; Inoue, T.; Harata, A.; Ogawa, T. *Langmuir* 1999, *15*, 8651-8658.

60. Peterson, E. S.; Harris, C. B. *J. Chem. Phys.* 1989, *91*, 2683-2688.

61. Xu, Z.; Dong, Y. *Surf. Sci.* 2000, *445*, L65-L70.

62. Simpson, G. J.; Westerbuhr, S. G.; Rowlen, K. L. *Anal. Chem.* 2000, *72*, 887-898.

63. Selwyn J. E.; Steinfeld, J. I. *J. Phys. Chem.* 1972, *76*, 762-774.

64. Rohatgi K. K.; Mukhopadhyay, A. K. *Photochem. Photobiol.* 1971, *14*, 551-559.

65. Adamson, A. W. *Physical Chemistry of Surfaces, 4th ed.*; Wiley: New York, 1982.

66. Rosen, M. J. *Surfactants and Interfacial Phenomena*; Wiley: New York, 1978.

67. Dick, B.; Gierulski, A.; Marowsky, G.; and Reider, G.A. *Appl. Phys. B* **1985,** 38, 107-116.

68. Guyot-Sionnest, P.; Shen, Y. R.; Heinz, T. F. *Appl. Phys. B* 1987, *42*, 237-238.

69 Dick, B. *Chem. Phys.* 1985, *96*, 199-215.

70. These results are similar to those reported by Haslam et al.[51] for PNP and TPB at the dodecane/water interface. A Frumkin isotherm can be used as an alternate analysis.

71. Note that the change is K_d is not the same as the change in [D] since the latter depends upon the added dye concentration [M_o]. For M_o close to K_d, [D] increases by about a factor of 2.

72. It is also possible that the absolute, if not relative, values for the hyperpolarizibilities vary with composition. (The relative ones, given by β_r, from the polarization studies, were found to be fairly insensitive to changes in the solution). The dimer structure could vary with solution composition or higher aggregates could be formed. These

processes would be accompanied by a larger variation in the polarization dependence than we observe. The formation of large aggregates appears to be more prevalent for J-aggregates, such as those for cyanine dyes ([Spano; Mukamel, *Phys. Rev. A* 1989, *40*, 5783-5801], [Weigand; Rotermund; Penzkofer, *Chem. Phys.* 1997, *220*, 373-384]), than for H-aggregates.

73. The band widths for the linear solution and SHG spectra are more similar for OX720 because there is a higher fraction of dimers in this case.

74. Marowsky, G.; Gierulski, A.; Dick, B. *Optics Comm.* 1985, *52*, 339-342.

75. The cationic dyes can have several charge states; it is unlikely that the charge is altered at the surface based on the large spectral shifts measured by Gvishi, Reisfeld, and Eisen [*Chem. Phys. Lett.* 1989, *161*, 455 – 460] for the neutral and dicationic forms of nile blue.

76. Kemnitz, K.; Tamai, N.; Yamazaki, I.; Nakashima, N.; Yoshihara, K. *J. Phys. Chem.* 1986, *90*, 5094-5101.

77. Note that for the studies carried out for dyes on silica, the substrates are not very polar so that it is relatively easy for intermolecular interactions to raise the polarity. The polarity of water is certainly higher and although at the interface it is lower than bulk water, it is probably more difficult to raise the medium polarity at the water surface through adsorbate interactions than it is on silica.

78. Monomeric species are obviously more likely to be found at the surface if they are insoluble. There have been many previous studies of insoluble organic molecules at

interfaces, such as for Langmuir-Blodgett films, in which the monomer is detected at the surface.

Tables

Table 1 – Peak positions and K_d for the oxazine dyes[a]

	Solution			*Surface*	
Dye	ν_M / nm	ν_D / nm	K_d / M [b]	ν_{SHG} / nm	$\Delta\nu$ / nm
oxazine 720[e]	620	570	2.0×10^{-5}	569	88
			$2.0 \pm 0.5 \times 10^{-5}$ [c]		
			10^{-4} - 10^{-5} [d]		
cresyl violet	580	550	3.1×10^{-4}	574	76
nile blue	630	590	1.0×10^{-4}	597	79

[a] Solution values are for dye solutions without salt. Surface values are from SHG measurements for the salted solutions shown in Figure 3. Band center wavelengths (in nm) for solutions with salt are: NB 635 (monomer) and 590 (dimer), CV 590 (monomer) and 550 (dimer), OX720 620 (monomer) and 565 (dimer).

[b] The uncertainties in K_d are estimated to be ± 30%. Compared to the solutions without salt, the K_d with salt were found to be lower by a factor 2 for OX720 and 3 for NB and CV.

[c] Reference 37.

[d] Reference 35.

[e] Using Triton X to determine K_d yields a value of 1.9 x 10^{-5} M.

Table 2 – ΔG_{ad} for oxazine dyes with and without salt added

	ΔG_{ad} / (kcal mol^{-1})[a]	
Dye	w/o salt	w/ salt
oxazine 720	- 10.4	- 14.6
nile blue	- 9.7	- 14.1
cresyl violet	-	- 9.6

[a] The uncertainty in ΔG_{ad} is ±1 kcal/mol.

Table 3 – Results from the SHG polarization dependence measurements for oxazines at the air/water interface[a]

	[NaCl] / M	$\frac{I_{pp}}{I_{ps}}$	$\frac{I_{s,45}}{I_{ps}}$	$\frac{\chi_{zzz}}{\chi_{zxx}}$	$\frac{\chi_{xxz}}{\chi_{zxx}}$	$\delta = 45°$, random [b]		$\delta = 0°$ [b]		β_r	ξ/deg
						D	θ/deg	D	θ/deg		
nile blue	0	0.45	0.023	0.14	0.20	0.91	17.2	0.96	12.1	0.25	77.9
	0.01	0.58	0.0081	0.18	0.12	0.88	20.3	0.94	14.2	0.19	75.8
oxazine 720	0	0.63	<0.054	0.33	0.31	0.84	23.4	0.92	16.3	0.41	73.7
	0.1	0.55	0.018	0.26	0.18	0.85	22.5	0.93	15.7	0.27	74.3
cresyl violet	0	0.81	<0.051	0.43	0.30	0.81	26.0	0.90	18.0	0.42	72.0
	0.1	0.70	<0.051	0.37	0.30	0.83	24.5	0.91	17.0	0.41	73.0

a. See text for details concerning the analysis. The dye concentrations were in the range $5 \times 10^{-5} - 2 \times 10^{-4}$ M. All measurements were conducted with the ultrafast laser system and at an incident angle of 60° except for oxazine 720 with salt for which the results listed were obtained with the picosecond OPA system at an angle of 40°.

b. For $\delta = 45°$ or for a random distribution, $Y = 1$, and for $\delta = 0°$, $Y = 2$. Y is a coefficient that appears in the equation for the orientation parameter D that depends on the assumed nature of the orientation distribution for δ, the angle of rotation about the z-axis. $\delta = 0°$ corresponds to the y-axis parallel to the surface.[54]

Figure Captions

Figure 1 – Molecular structure of oxazine dyes

Figure 2 – Illustration of monomer / dimer striping procedure for nile blue described in the text. The dot – dash line is the extinction spectrum for the monomer (ε_M) obtained at 2.0×10^{-6} M. The dimer extinction ($\varepsilon_D/2$, dashed line) was obtained by subtracting $(1 - x)\varepsilon_M$ from a spectrum measured at 3.8×10^{-5} M (open circles). The dimer spectrum and K_d from x were used to model (solid line) the curve for 9.2×10^{-6} M (closed circles). See Table 1 for results.

Figure 3 – SHG spectra and linear absorbance spectra for a) nile blue, b) cresyl violet, and c) oxazine 720. The closed circles are the data and the dashed line is the curve based on a fit to a Gaussian. The solid and dot – dash lines are linear spectra for the visible and UV regions respectively, where the latter is plotted on the upper wavelength scale.

Figure 4 – Langmuir isotherms measured for NB a) with and b) without salt in the solutions. The SHG intensities are plotted as a function of the dimer concentration calculated from the added dye and K_d. In the inset of a), the data is plotted as a function of the input monomer concentration. The inset of b) is plotted on an expanded concentration range which shows that the signal reaches a maximum and decreases. The values obtained for ΔG_{ad} can be found in Table 2.

Figure 5 – Polarization dependence of SHG intensities: a) OX720 with 0.1 M NaCl and b) nile blue. The closed and open circles represent the I_p and I_s data respectively and the solid lines are from the analysis using equation 7. The I_s data in b) is multiplied by a factor of 10 for presentation.

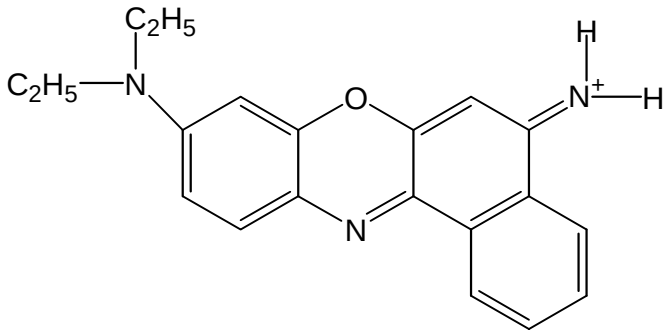

Nile Blue

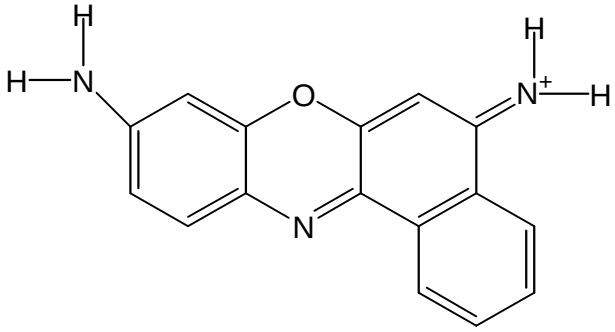

Cresyl Violet

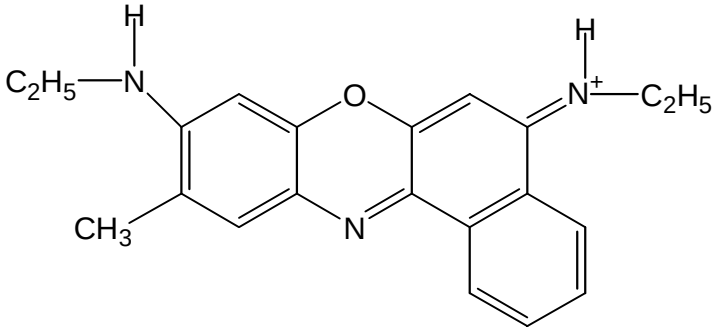

Oxazine 720

Figure 1

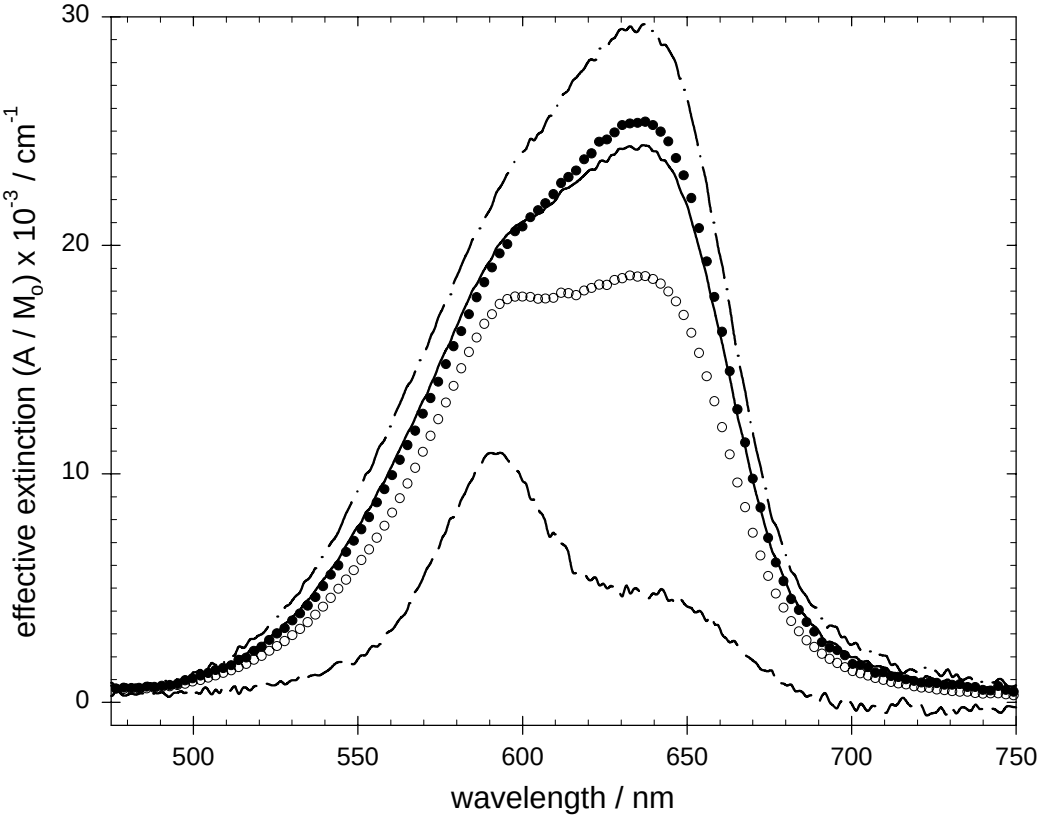
30
20
10
0
500
550
600
650
700
750
effective extinction (A / M$_o$) x 10^{-3} / cm^{-1}
wavelength / nm

Figure 2

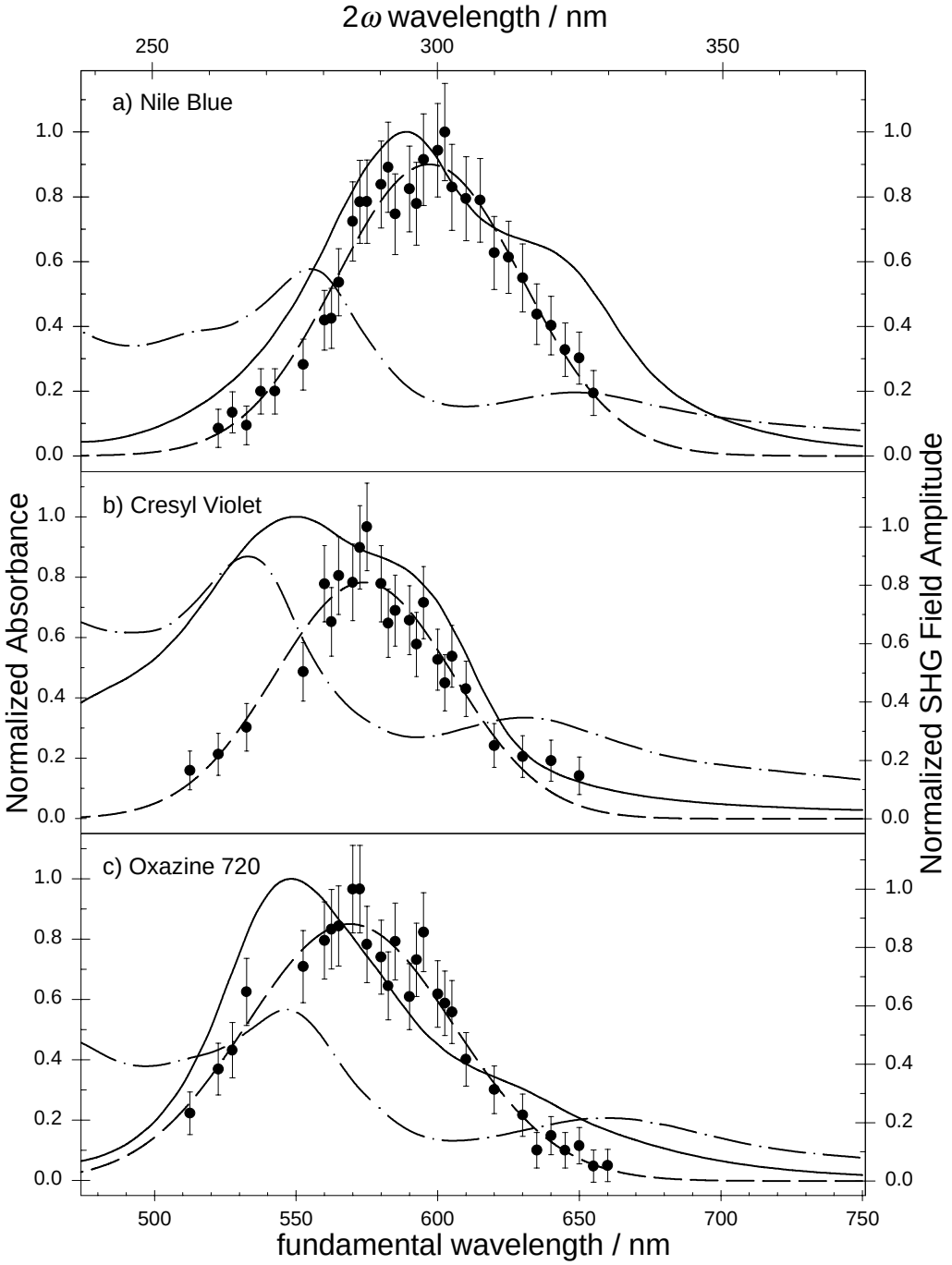
2ω wavelength / nm
250
300
350
a) Nile Blue
b) Cresyl Violet
c) Oxazine 720
Normalized Absorbance
Normalized SHG Field Amplitude
0.0
0.2
0.4
0.6
0.8
1.0
500
550
600
650
700
750
fundamental wavelength / nm

Figure 3

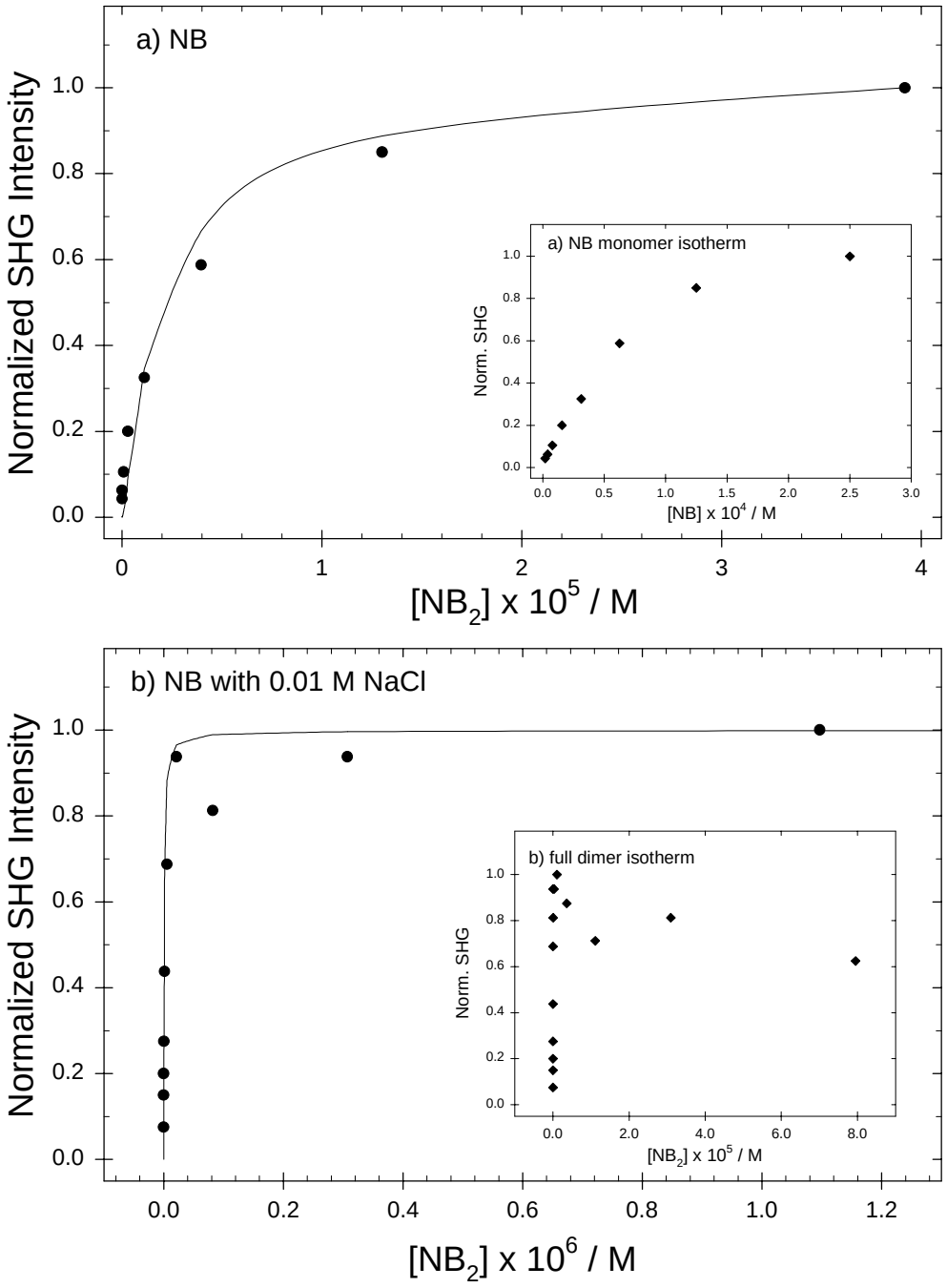
a) NB
Normalized SHG Intensity
[NB2] x 10^5 / M
a) NB monomer isotherm
Norm. SHG
[NB] x 10^4 / M
b) NB with 0.01 M NaCl
Normalized SHG Intensity
[NB2] x 10^6 / M
b) full dimer isotherm
Norm. SHG
[NB2] x 10^5 / M

Figure 4

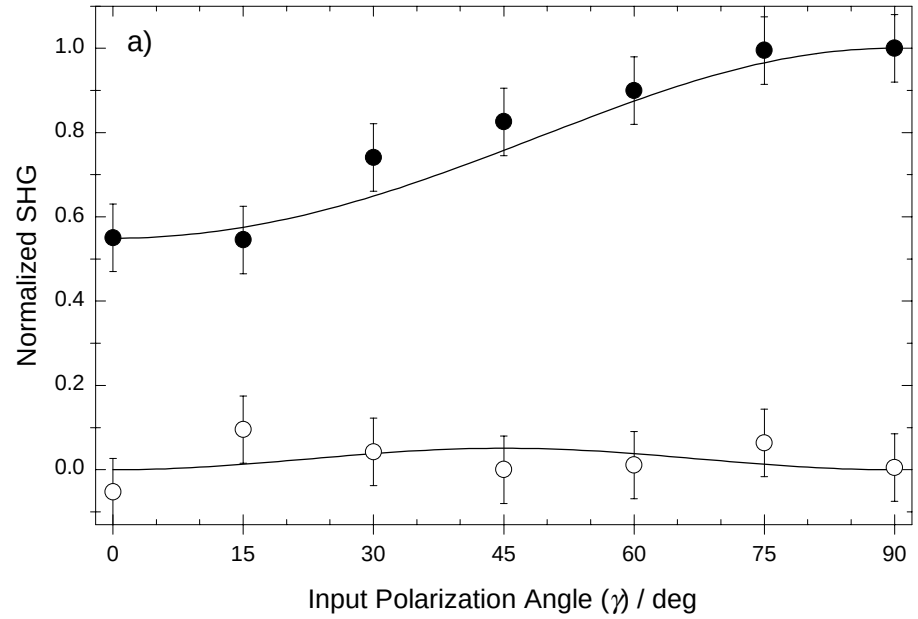
a)
Normalized SHG
1.0
0.8
0.6
0.4
0.2
0.0
0
15
30
45
60
75
90
Input Polarization Angle (γ) / deg

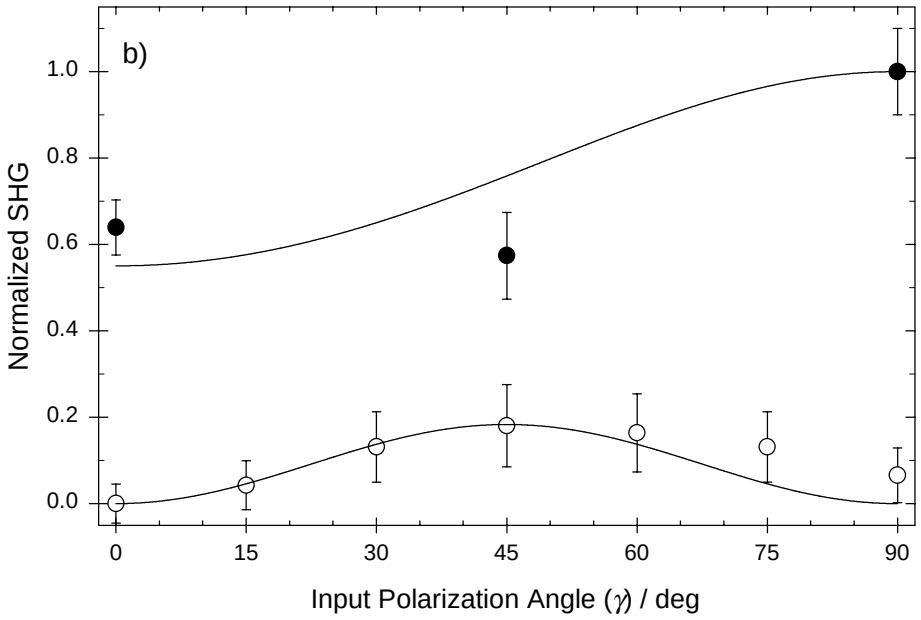
b)
Normalized SHG
1.0
0.8
0.6
0.4
0.2
0.0
0
15
30
45
60
75
90
Input Polarization Angle (γ) / deg

Figure 5